

# Microstructure of AA2024-SiC nanostructured metal matrix composites

Timothy (Zhigang) Lin · Chunhu Tan ·  
Bob Liu · Adolphus McDonald

Received: 12 March 2008 / Accepted: 12 May 2008 / Published online: 21 July 2008  
© Springer Science+Business Media, LLC 2008

**Abstract** Nanostructured metal matrix composites (NMMCs) in large-dimension billets were fabricated by hot isostatic pressing (HIPing) of cryomilled powders consisting of AA2024 alloy reinforced by 25 wt.% SiC particles. Microstructure of the bulk nanostructured composites and cryomilled powders was characterized by X-ray diffraction (XRD), scanning electron microscopy (SEM), and transmission electron microscopy (TEM). In addition, mechanical properties of the bulk nanocomposites were also addressed.

## Introduction

Metal matrix composites (MMCs) typically based on Al alloys are currently the materials of choice for many lightweight structural applications. Recent development in nanocrystalline (NC) metals and alloys, with average and range of grain sizes typically smaller than 100 nm, has attracted considerable research interest in seeking a new opportunity for substantial strength enhancement of materials. This is primarily due to superior mechanical properties found in this class of materials, including high strength and high toughness [1]. For lightweight structure applications requiring high strength, an increase in material strength consequently leads to a reduction of structure

weight. However, the major roadblock to NC's structural applications is the difficulty in fabricating them into bulk forms. Toward this end, much research has so far focused on the synthesis of bulk NC metals and alloys using a variety of techniques [2–4]. Recent studies have demonstrated that it is feasible to attain bulk NC metals/alloys and composites [4].

The present study is to understand the size, distribution, and morphology of matrix grains and reinforcement particles in a large-dimension billet of nanostructured AA2024-SiC MMC, which was developed for lightweight, ultra-high strength ballistic armor applications. The nanostructured MMC was fabricated via consolidation of cryomilled powder composite with nanometer-sized grains. It is important to characterize the microstructure of the composite to understand the formation of the nanometer-sized microstructure and hence to enhance the mechanical properties. We characterized the microstructure of consolidated billet in large dimension by X-ray diffraction (XRD), scanning electron microscopy (SEM), and transmission electron microscopy (TEM).

## Materials and experiments

Large-dimensional AA2024-SiC billets were fabricated from cryomilled powder composite. Commercial AA2024 Al alloy powders from Valimet Inc. (Stockton, CA) and SiC powders from Atlantic Equipment Engineering (Bergenfield, NJ) were used as the starting materials for mechanical milling at cryogenic temperature (cryomilling [5]). The composition of the raw 2024 Al alloy powder used is 4.35 pct Cu, 1.50 pct Mg, 0.60 pct Mn, 0.15 pct Zn, 0.10 pct Cr, 0.25 pct Fe, 0.45 pct Si, 0.08 pct O, and with the remaining as Al. The diameter of SiC particles was sub- $\mu\text{m}$  to several  $\mu\text{m}$ . The blend of 75 wt.% 2024 Al alloy

T. Lin (✉) · C. Tan · B. Liu  
Aegis Technology Inc., 3300 A Westminster Ave., Santa Ana,  
CA 92703, USA  
e-mail: timlin@aegistech.net

A. McDonald  
U.S. Army Aviation and Missile Command, Bldg. 5400,  
Redstone Arsenal, AL 35898, USA

powders and 25 wt. % SiC powders was milled in liquid nitrogen using an attritor with a capacity of 15 lb per batch. The cryomilled powders were then degassed at elevated temperature up to 350 °C until the canned powder reaching a vacuum less than  $10^{-6}$  Torr. After degassing, the cryomilled AA2024-25 wt.% SiC powders were consolidated by using Hot Isostatic Pressing (HIPing) at 410 °C to produce large-dimension billets with a diameter of 6–8 inch and thickness of 1–2 inch.

Figure 1 shows some typical billets produced (Fig. 1a), and the associated microstructure (Fig. 1b). Figure 1b is the cross-sectional image using optical microscopy to evaluate the overall soundness and uniformity of the microstructure in a typical bulk AA2024-SiC composite sample. It was found to be well consolidated in most areas, and no noticeable pore/voids were observed in optical microscopy, indicating the accomplishment of good densification during the HIPing process. The distribution of SiC particles, which were identified as gold color on the optical images, was uniform in general, although some of the SiC particles observed are very large ( $>10\ \mu\text{m}$ ), which were presumably from the starting powders.

In order to carry out more intricate microstructure examination of the NMMCs, both in the stage of cryomilled powders and consolidated bulk billets, several advanced microstructural analysis methods were employed. Scanning electron microscopy (SEM) observation was performed on a Philips XL 30 microscope with a field emission gun. X-ray

diffraction (XRD) measurements were carried out with a Siemens D5000 diffractometer equipped with a graphite monochromator using Cu  $K_{\alpha}$  radiation. Transmission electron microscopy (TEM) observations were carried out with a Philips CM20 microscope operated at 200 kV.

## Results and discussion

The cryomilled powders consist of nanostructured composite. The milled particles were about 10  $\mu\text{m}$  to 120  $\mu\text{m}$ , and were agglomerated with an irregular-shaped feature indicative of severe deformation caused by the ball milling process. Representative SEM images of cryomilled powders are shown in Fig. 2a. Figure 2b shows the ultra-fine particles embedded in a large agglomerated particle. EDX results of the particles indicated that the main elements in the particle are Al, Cu, Si and C, in agreement with the overall composition of the composite.

TEM observations revealed grain sizes in the cryomilled powders are typically in the range from  $\sim 10\ \text{nm}$  to 50 nm. Representative images are displayed in Fig. 3a (bright field image) and b (dark field image). The nanometer-sized Al grains were found to be uniform in the area observed. It is clear that the nanometer-sized grain microstructure formed after the cryomilling. The ring diffraction pattern is shown in Fig. 3c. The D-spacing values of the first four clear rings were found to be close to those of  $\alpha$ -Al's (111), (200), (220),

**Fig. 1** (a) Photo of AA2024-SiC prototype billets; (b) optical image showing typical microstructure in the prototype fabricated by HIPing

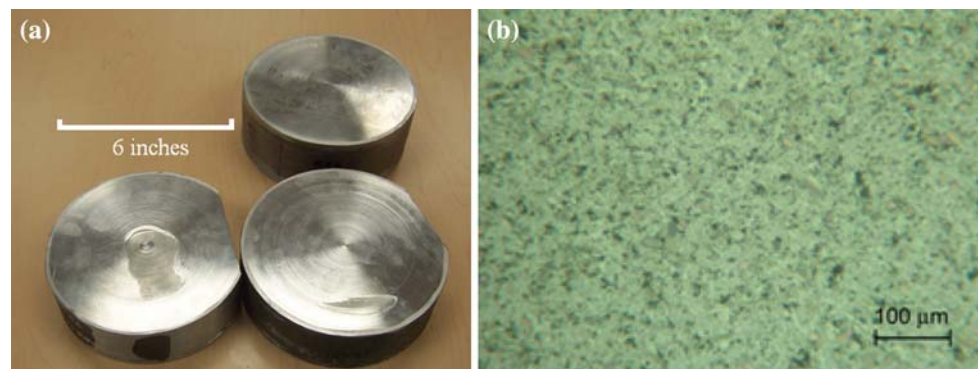


**Fig. 2** (a) Representative SEM image of cryomilled AA2024-25%SiC nanocomposite powders; (b) magnified image of a typical agglomerated particle as shown in (a)

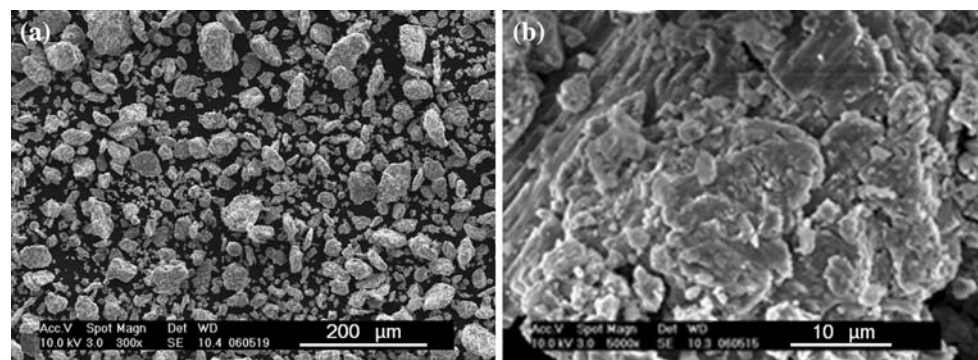


**Fig. 3** TEM images of cryomilled AA2024-25%SiC powder sample: (a) bright field image; (b) dark field image (taken with  $(111)_{Al}$  beam); (c) selected electron diffraction pattern; (d) EDS spectrum (taken from the whole particle area shown in Fig. 3a and b)

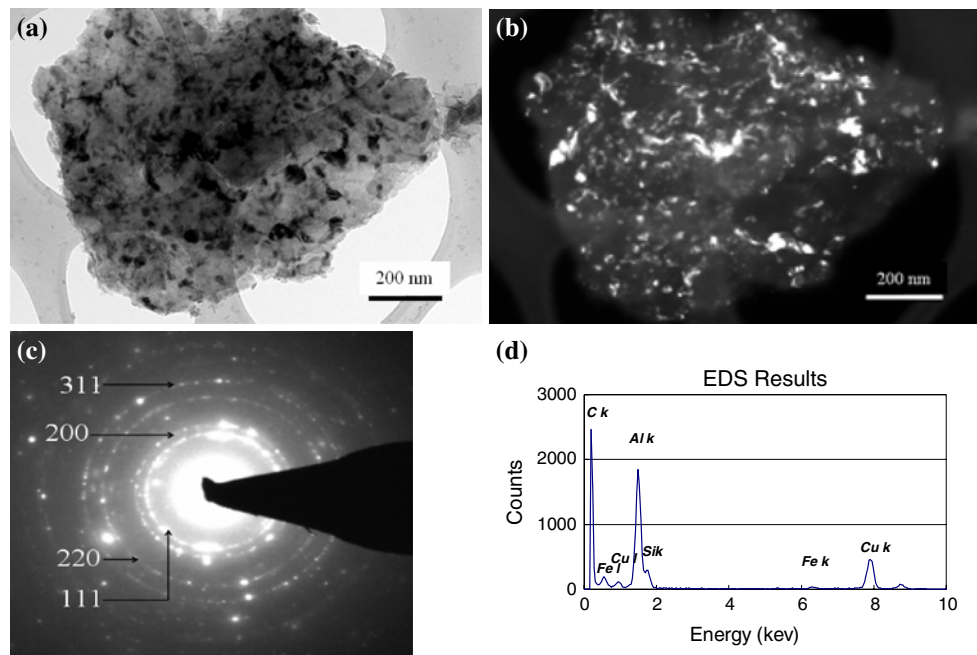
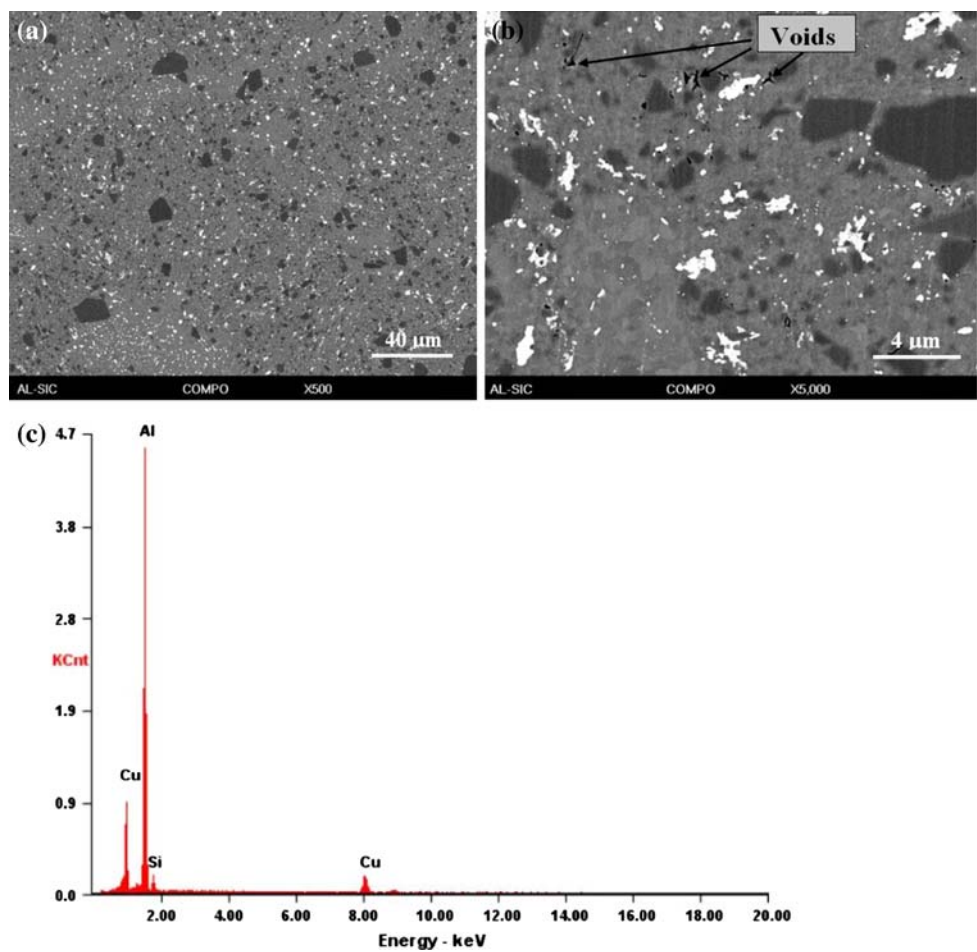


**Fig. 4** Representative SEM images showing the cross-sectional microstructure of bulk nanostructured AA 2024Al-SiC composite: (a) showing the regions of good consolidation and good uniformity; (b) showing the region with porosity (black feature) and non-uniform grain structure; (c) EDX pattern of the bright particles



and  $(311)$ . Figure 4d is the obtained X-ray diffraction result identifying Al as the major element in the area (another one is Cu).

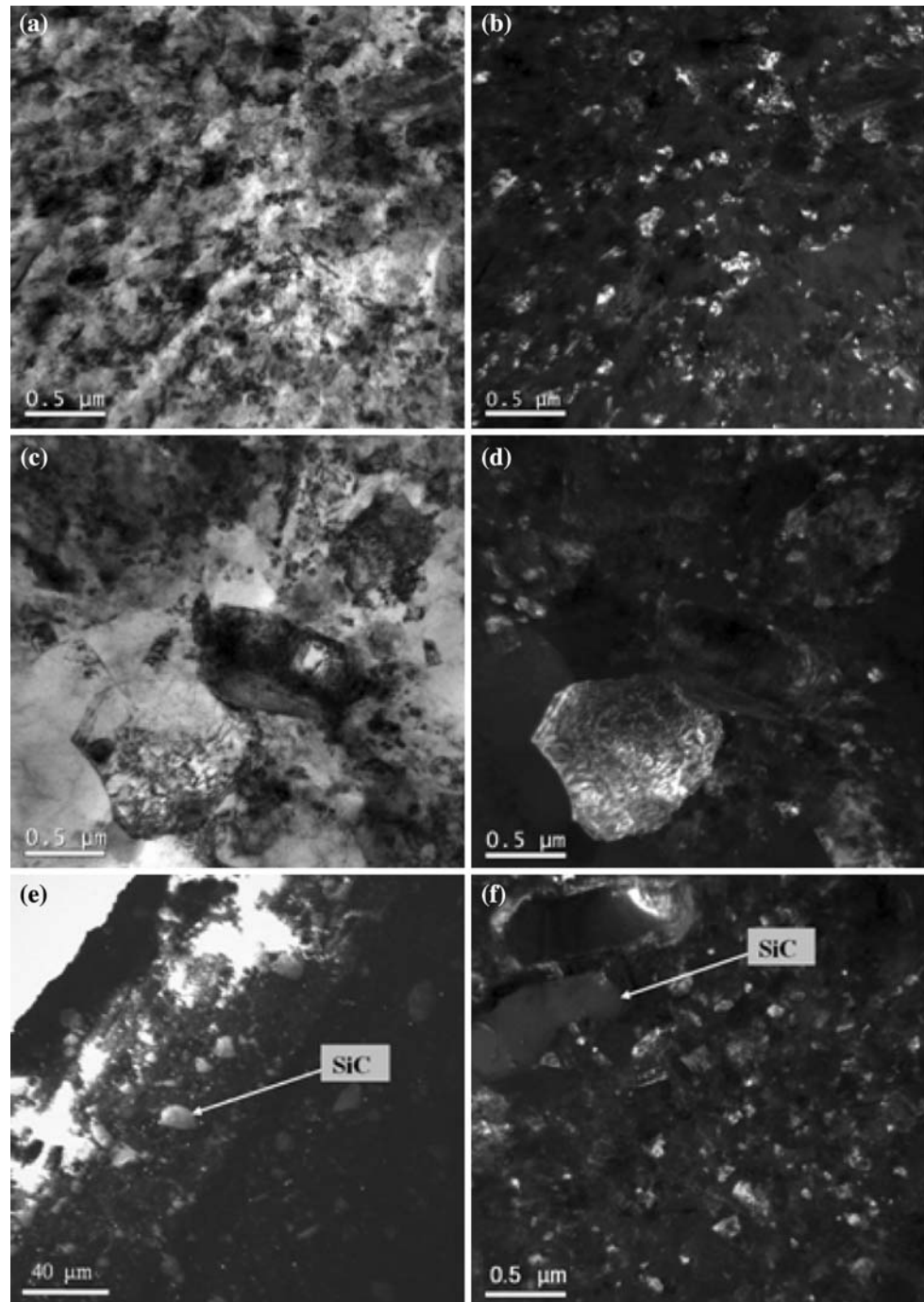
In addition, XRD measurement of the cryomilled powder composite indicated reflection peaks of both AA2024 Al alloy (i.e.,  $\alpha$ -Al phase) and SiC. The average grain size

of  $\alpha$ -Al phase estimated using the Scherrer formula based on the peak broadening was about 25 nm, which is in good agreement with the TEM observation. The grain size results are consistent with those reported for milled Al metal and alloys [2, 6].

Consolidated AA2024-SiC composite samples were examined using SEM to evaluate the uniformity of the microstructure and the grain/particle sizes. The representative cross-sectional images are displayed in Fig. 4. Figure 4a reveals a homogeneous distribution of the particles

embedded in a matrix. Based on the size and morphology feature, one may conclude that the dark particles are SiC. Most SiC particles were found to be less than 5  $\mu\text{m}$ . However, particles as large as 10  $\mu\text{m}$  were also observed. The distribution of SiC particles and Al-Cu intermetallic phases, which were identified as dark and bright particles in the SEM images, was uniform in general. Moreover, SEM observations (Fig. 4b) with high magnification revealed the presence of small voids in some areas, though in most regions, no micro-voids or porosity were detected. In addition, the grain

**Fig. 5** Representative TEM images showing the typical grain structure in a consolidated bulk AA2024-25%SiC sample: (a) bright field image of nanometer-sized grains; (b) dark field image of nanometer-sized grains; (c) bright field image of large grains; (d) dark field image of large grains; (e) Large SiC particles of about 10  $\mu\text{m}$ ; (f) small SiC particles of about 1  $\mu\text{m}$  (dark field image)



structure appears to be non-uniform, in which some large grains are in the range of sub- $\mu\text{m}$  or even close to about 1  $\mu\text{m}$ . EDX results indicated that the bright particles were Al–Cu and the dark ones were SiC. A representative EDX pattern is presented in Fig. 4c.

In order to further characterize the microstructure of the bulk composite, TEM observations were conducted. In general, the grain size and distribution were found to be non-uniform in the consolidated samples. Representative images are displayed in Fig. 5. Two types of grain feature were observed. The first type is nanometer-sized in the range of 20–100 nm, as represented by the region shown in Fig. 5a and b. These grains were typically equiaxed and much larger compared to the cryomilled powder. In addition to these ultra-fine grains, much coarse grains in the form of bands or clusters, in the range of sub- $\mu\text{m}$  to 1  $\mu\text{m}$ , were also observed in some areas, as shown in Fig. 5c and d. In Fig. 5e and f, SiC particles with sizes of about 10  $\mu\text{m}$  and about 1  $\mu\text{m}$  were observed in the Al matrix.

The non-uniform, bi-modal grain size distribution observed in the present bulk composite was primarily due to the recrystallization and grain coarsening at elevated temperatures [6, 7] during the degassing and HIPing processes. Similar results were reported previously in Al alloys [8] and Al composite reinforced by SiC [9].

The mechanical performance of the AA2024–SiC prototypes was also obtained by using a uni-axial compression test with specimen dimension of 4 mm  $\times$  4 mm  $\times$  8 mm, randomly cut directly from HIPed prototypes (generally 150–200 mm in diameters), for instance, at the edge areas of prototypes as shown in Fig. 1. The typical ultimate strength for the HIPed prototypes of AA2024–25%SiC NMMC is generally in the range of 92 ksi ( $\sim$ 635 MPa) to 102 ksi ( $\sim$ 705 MPa) with the ductility in the range of 4–8%. A representative compressive stress–strain curve is displayed in Fig. 6, showing the strength of about 97 ksi ( $\sim$ 670 MPa) and fracture strain of about 4.7%.

Finally, it should be pointed out that the observed microstructure characteristics that are described above are believed to contribute primarily to the mechanical properties of the large bulk, ultrafine-grained composite, which exhibited ultimate compression strength in the magnitude of 700 MPa. Although the strength is higher than commercially available high-strength Al alloy and SiC reinforced composites, it is still desirable to achieve a much higher strengthening effect due to the grain refinement. It is believed that the failure to achieve the strength much higher than 700 MPa may primarily result from the presence of micro-voids or porosity in the bulk billet, as indicated in the previous Fig. 4. The macro-fractography also indicated that the fracture sources were micro-voids resulting from locally insufficient consolidation, which may be related to the oxidation of the cryomilled powders and/or inevitable

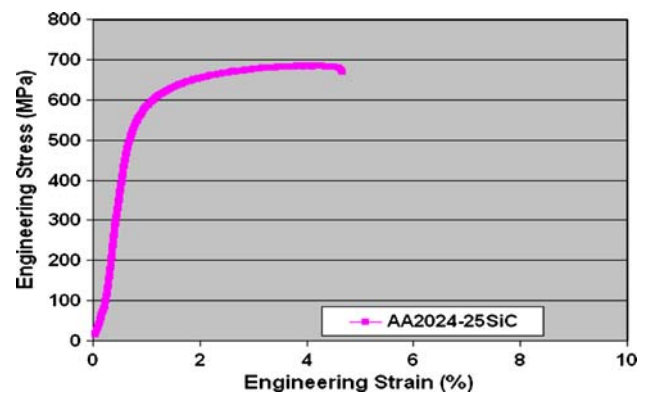


**Fig. 6** Typical compressive stress–strain curve of AA2024–25%SiC NMMC prototype

contamination sources from the steel balls or other steel components in the attritor. In addition, the utilization of a proper secondary consolidation process such as extrusion or forging would further improve the strength. The work in this aspect is still ongoing.

## Summary

Large quantity (15 lbs/batch) AA2024–25 wt.%SiC powder composites, consisting of nanostructured Al matrix (e.g.,  $\alpha$ -Al phase) with a grain size of about 25 nm and micrometer-sized SiC particle, were produced via cryomilling. In the large-dimension billets, by consolidating the cryomilled powder composites with a HIPing process, the growth of nanometer-sized grains was found to be limited, and the Al matrix was found with a non-uniform size distribution that includes both equiaxed, nanometer-sized grains in the range of 20–100 nm and coarse-grain zone with grains in the range of sub- $\mu\text{m}$  to 1  $\mu\text{m}$ . The presence of micro-voids/porosity in the large bulk billet is believed to be the failure source leading to a less strengthening effect anticipated from the grain refinement in nanometer to sub- $\mu\text{m}$  scale. Further optimization of consolidation process and/or using a proper secondary consolidation process such as extrusion or forging would further improve the strength.

**Acknowledgement** This work was supported by US Army Research and Engineering Command under a SBIR fund (Contract No. W911W6-06-C-0032).

## References

1. Kumar KS, Van Swygenhoven H, Suresh S (2003) *Acta Mater* 51:5743. doi:10.1016/j.actamat.2003.08.032
2. Koch CC (1997) *Nanostruct Mater* 9:13. doi:10.1016/S0965-9773(97)00014-7

3. Valiev RZ, Islamgaliev RK, Alexandrov IV (2000) *Prog Mater Sci* 45:103. doi:[10.1016/S0079-6425\(99\)00007-9](https://doi.org/10.1016/S0079-6425(99)00007-9)
4. Witkin D, Han BQ, Lavernia EJ (2006) *Metall Mater Trans A37*:185. doi:[10.1007/s11661-006-0163-2](https://doi.org/10.1007/s11661-006-0163-2)
5. Luton MJ, Jayanth CS, Disko MM, Matras S (1989) *Vallone J Mat Res Soc Symp Proc* 132:79
6. Zhou F, Liao XZ, Zhu YT, Dallek S, Lavernia EJ (2003) *Acta Mater* 51:2777
7. Zhou F, Lee J, Dallek S, Lavernia EJ (2001) *J Mater Res* 16:3451. doi:[10.1557/JMR.2001.0474](https://doi.org/10.1557/JMR.2001.0474)
8. Newbery AP, Nutt SR, Lavernia EJ (2006) *JOM* 4:56. doi:[10.1007/s11837-006-0216-4](https://doi.org/10.1007/s11837-006-0216-4)
9. Tang F, Hagiwara M, Schoenung JM (2005) *Mater Sci Eng A* 407:306. doi:[10.1016/j.msea.2005.07.056](https://doi.org/10.1016/j.msea.2005.07.056)